

Simulation Study of Natural Gas Blending with Hydrogen and Dissociated Methanol Gas for Boiler Combustion

Weihong Xu¹, Ruhuan Jiang¹, Lunhong Chen², Yankun Jiang^{1,3,*}

¹*School of Energy and Power Engineering, Huazhong University of Science and Technology, Wuhan, Hubei, China*

²*Hubei Huayang Automobile Transmission System Co., Ltd, Shiyan, Hubei, China*

³*State Key Laboratory of Coal Combustion, Huazhong University of Science and Technology, Wuhan, Hubei, China*

**Corresponding Author.*

Abstract: In light of the worldwide consensus on net-zero emissions, using clean fuels to wholly or substantially replace traditional fuels has emerged as the dominant route of industrial development. This paper presents a methanol-hydrogen co-combustion method for boilers, based on methanol, a zero-carbon fuel produced from CO₂. The technique uses boiler waste heat to catalytically fracture methanol into dissociated methanol gas (DMG), largely composed of H₂ and CO. The DMG is blended with the original fuel to improve thermal efficiency and minimize emissions. A three-dimensional geometric model was developed with a tiny direct-current natural gas (NG) boiler as the research subject. The combustion characteristics of natural gas mixed with various concentrations of DMG and hydrogen were simulated using the finite volume approach. Blending hydrogen and DMG at a flow rate of 10 m³/h and a surplus air ratio of 1.2 improves the NG heat release rate and furnace temperature. At a 5% hydrogen mixing ratio, the heat release rate rises by up to 2.2%, while the average furnace temperature reaches a high of 1886 K. Meanwhile, at a DMG mixing ratio of 10%, the heat release rate increases by a maximum of 2.1%, while at a mixing ratio of 5%, the average furnace temperature reaches 1895 K. Overall, hydrogen has a greater effect on increasing the heat release rate of NG combustion, whereas DMG has a larger potential to raise furnace temperature.

Keywords: Boiler; Natural Gas; Hydrogen; Dissociated Methanol Gas; Combustion Simulation;

1. Introduction

As the worldwide consensus on net-zero emissions grows and countries implement increasingly rigorous energy conservation and emission reduction targets, the partial or complete replacement of traditional fuels with clean alternatives has emerged as the main trend in industrial development. Boilers, which run largely on fossil fuels like coal, oil, and natural gas (NG), produce large amounts of carbon dioxide and other gaseous pollutants during combustion. Furthermore, the release of smoke, trace heavy metals, and other hazardous compounds endangers the health and survival of humans, animals, and plants. [1,2] As a result, green and low-carbon transformations and upgrades to boiler equipment are critical to achieving carbon neutrality.

Coal and biomass can be used to make methanol, which is abundant and inexpensive. When thermally decomposed, it produces hydrogen, making it an excellent hydrogen carrier with vast application possibilities and substantial benefits over other renewable energy sources. [3,4] Green methanol made from CO₂ is virtually a zero-carbon fuel. [5,6] Methanol has 50% more oxygen than natural gas (NG), the major fuel for small industrial boilers, allowing for complete combustion, increasing the fuel's heat release rate, and improving energy system thermal efficiency. Promoting methanol as a partial or full replacement for NG as a fuel for gas boilers helps to increase clean energy usage in small industrial boilers.

Existing research is mostly concerned with using hydrogen as a partial alternative for natural gas (NG) in boilers. Liu et al. [7]

investigated the combustion parameters of NG and hydrogen mixtures in a residential swirl furnace using hot-state tests and numerical analysis. Their findings revealed that when NG is blended with 15% hydrogen by volume, CO emissions drop by 25% and the average combustion zone temperature falls by 6.7%, proving the viability of methane-hydrogen mixtures as fuels in household swirl furnaces. Balanescu et al. [8] investigated the carbon emission reduction and latent heat recovery capabilities of condensing boilers powered by methane-hydrogen mixtures. They used the Ostwald diagram to compute the maximum concentrations of CO₂ and CO in flue gases, as well as the water vapor partial pressure and dew point temperature, as the hydrogen volume fraction climbed from 0% to 100%. The results showed that increasing the hydrogen component in the fuel mixture increased the condensing boiler's thermal efficiency by up to 1.3%. Sun et al. [9] studied how NG combined with 0%, 5%, 10%, 15%, and 20% hydrogen by volume affected the performance of residential gas stoves. Their research found that increasing hydrogen content decreased flame length, increased thermal efficiency, and reduced CO and NO_x emissions. At 20% hydrogen volume percentage, CO₂ emissions decreased by 9.33%. However, when the hydrogen concentration in gas water heaters reached 23%, there was evident backfiring. These investigations show that hydrogen is frequently used for combustion directly from tank storage, which presents storage, transportation, and safety difficulties [10]. In contrast, methanol is a liquid at room temperature. Directly integrating methanol into NG boilers necessitates structural optimization of burners, which raises costs.

To address these technical issues concurrently, the authors suggest a methanol-hydrogen co-combustion technique. The process involves using boiler waste heat to evaporate methanol into vapor, which is then catalytically broken into dissociated methanol gas (DMG), largely consisting of H₂ and CO. DMG is blended directly with NG to improve boiler thermal performance and reduce emissions [11,12]. DMG has a larger volumetric calorific value than pure hydrogen and is more cost-effective [13,14]. For calculations, DMG is regarded as an ideal gas with a volume ratio of H₂ to CO of

2:1 in the following analysis.

The research focuses on developing a three-dimensional geometric model of a small direct-current NG boiler as the study subject, as well as simulating the effects of blending NG with varying proportions of DMG and hydrogen on the furnace's heat release rate, flue gas exit velocity, peak temperature, average temperature, and flue gas exit temperature using the finite volume method. This research seeks to provide theoretical direction for the subsequent optimization of methanol-hydrogen boiler furnaces.

2. Model Description

A three-dimensional solid model of the boiler was generated using SpaceClaim throughout the research phase, which was based on the Ansys platform. Fluent meshing was then used to discretize the model, yielding a hybrid-type volume mesh. Numerical simulations were then performed using Fluent to investigate crucial parameters such as the flow characteristics and temperature distribution of the internal fluid, providing strong support for the boiler's optimization design.

2.1 Fundamental Governing Equations

Once the gas and air enter the furnace, complex flow, chemical reactions, and heat transfer processes take place. During the fluid mixing, combustion, and heat transfer processes, the gas combustion within the boiler must adhere to the fundamental governing equations, which include mass, momentum, energy, and species conservation [15].

2.1.1 Conservation of mass

In a closed system, the total amount of matter remains constant in any physical or chemical process. The flow and combustion processes must satisfy the conservation of mass equation [15], which is expressed as follows:

$$\frac{\partial \rho}{\partial \tau} + \frac{\partial(\rho u)}{\partial x} + \frac{\partial(\rho v)}{\partial y} + \frac{\partial(\rho w)}{\partial z} = S_m \quad (1)$$

In the equation:

ρ : represents the density of the gas within the furnace;

u, v, w : represents the components of the gas velocity vector in the $x, y,$ and z directions, respectively;

S_m : represents the source term.

2.1.2 Conservation of momentum

The flow process involves changes in the mass and velocity of fluid elements and must satisfy the law of conservation of momentum [15]. The momentum conservation equation is as follows:

$$\frac{\partial}{\partial t}(\rho u_i) + \frac{\partial}{\partial x_j}(\rho u_i u_j) = -\frac{\partial p}{\partial x_i} + \frac{\partial \tau_{ij}}{\partial x_j} + \rho g_i + F_i \quad (2)$$

In the equation:

p : represents the static pressure; τ_{ij} : represents the stress tensor;

g_i : represents the gravitational body force in the i direction;

F_i : represents the external body force in the i direction.

The stress tensor is given by the following equation:

$$\tau_{ij} = \left[\mu \left(\frac{\partial u_i}{\partial x_j} + \frac{\partial u_j}{\partial x_i} \right) \right] - \frac{2}{3} \mu \frac{\partial u_i}{\partial x_i} \delta_{ij} \quad (3)$$

2.1.3 Conservation of Energy

When heat exchange is present in the flow system, the law of conservation of energy must be satisfied. The fluid energy E consists of internal energy i , kinetic energy $K = \frac{1}{2}(u^2 + v^2 + w^2)$, and potential energy P . Since there is a relationship between internal energy i and temperature T , it can be expressed as $i = c_p T$, where c_p is the specific heat capacity. Therefore, the energy conservation equation, with temperature T as the variable, can be derived [15]. The energy conservation equation is as follows:

$$\frac{\partial(\rho T)}{\partial t} + \text{div}(\rho u T) = \text{div} \left(\frac{k}{c_p} \text{grad} T \right) + S_T \quad (4)$$

In the equation:

c_p : represents the specific heat capacity of the fluid;

T : represents the temperature;

k : represents the thermal conductivity of the fluid;

S_T : represents the viscous dissipation term.

2.1.4 Conservation of species

During combustion, the total amount of each chemical species in the fluid is conserved in any continuous process. Over time t , the mole fraction of chemical species m within the fluid remains unchanged at any point in space, and within any infinitesimal element of space, the moles of chemical species m entering the element minus the moles exiting are equal to the moles of species m that are either produced or consumed due to chemical reactions. The species conservation equation can be expressed

as:

$$\frac{\partial(\rho Y_m)}{\partial t} + \nabla \cdot (\rho n Y_m) = S_m \quad (5)$$

In the equation:

ρ : represents the fluid density;

n : represents the velocity vector of the fluid;

Y_m : represents the mole fraction of chemical species m ;

S_m : represents the number of moles of species m altered per unit mass of fluid per unit time due to chemical reactions.

2.2 Selection of the Simulation Model

Based on the simulation requirements, the appropriate simulation model is selected, as shown in Table 1.

Table 1. Model Selection

Category	Model
Turbulence Model	RNG k-ε Model
Radiation Model	DO Model
Combustion Model	Finite Rate Model
Reaction Mechanism	Oxidation mechanism with 28 species and 146 reaction steps

2.3 Establishment and Calibration of the Three-Dimensional Model

2.3.1 Model construction and mesh generation

The dimensions of the non-premixed burner installed in the test boiler were measured as follows: the diameter of the fuel inlet pipe is 0.04 m, the diameter of the air inlet pipe is 0.09 m, the outlet diameter of the fuel pipe is 0.002 m, and the air outlet is shaped like a circular ring with a difference of 0.011 m between the inner and outer diameters. Figure 1 and Figure 2 illustrate the burner's physical and model diagrams, respectively. To make computations easier, the furnace shape is estimated as a rectangular prism with a length of 0.31 m, width of 0.2 m, and height of 0.6 m. The burner is 0.15 m from the furnace's top, while the outlet on the right side measures 0.2 m wide and 0.05 m high. The front and rear outlets are 0.31 m wide and 0.15 m high.



Figure 1. Burner Outlet

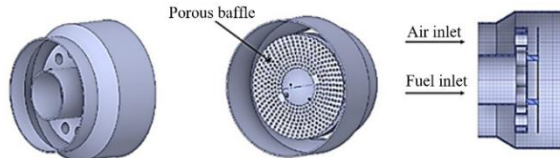


Figure 2. Three-Dimensional Model of the Burner

The simulation's accuracy is directly affected by the number of grids used. In theory, simulation accuracy is related to the number of grids: the more grids, the finer the mesh, and the better the local characteristics of the flow field can be recorded. However, once the grid count reaches a specific threshold, increasing the number of grids reduces accuracy while wasting processing resources.

Given the study's aims and computational efficiency, the construction of the combustion device was simplified, and the mesh was refined in locations with complex flow, such as the burner input and outlet. Figure 3 shows the total mesh partition of the burner and combustion chamber.

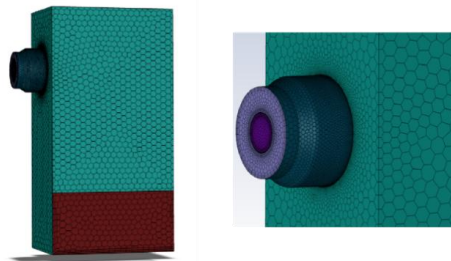


Figure 3. Boiler Mesh Model

2.3.2 Grid independence validation

Excessive meshing increases computing time and expense, but too few meshes might result in disappointing simulation results. In actual applications, it is critical to achieve a compromise between simulation accuracy and processing resources. By watching, comparing, and evaluating a certain parameter, the mesh quantity can be modified to attain the best outcomes.

Using natural gas (NG) as the boiler fuel, with a fixed flow rate of 10 m³/h, an excess air ratio of 1.2, turbulence intensity of 10%, and a hydraulic diameter of 0.038 m, the mesh size is modified to change the mesh count. Numerical simulations are carried out with identical initial circumstances and models with changing mesh quantities. When the furnace outlet temperature and pressure are stable, the combustion process is said to have reached a steady state, and the furnace outlet temperature is reported in Table 2.

Table 2. Impact of Mesh Quantity on Furnace Outlet Temperature

Mesh Quantity	Furnace Outlet Temperature (K)	Variation (1%)
415077	1899.27	—
486582	1907.26	4.2
543234	1913.55	3.3
642762	1915.38	1.0
724189	1916.32	0.5
793778	1915.90	0.2

The findings in Table 2 show that as the mesh quantity rises, the variation in furnace exit temperature reduces progressively. When the mesh quantity reaches 642,762, the temperature variation is less than 1%, which meets the results' accuracy standards. Given the significant computational resources required for such large mesh quantities, all future numerical computations are performed on the model with 642,762 meshes.

2.3.3 Validation of the numerical model

(1) The Test Bench Boiler

The experimental bench boiler is illustrated in Figure 4.



Figure 4. Experimental Boiler

The fundamental parameters of the boiler include evaporation rate (t/h), outlet steam pressure (MPa), outlet steam temperature (°C), and feedwater temperature (°C), which together define the key performance characteristics of the boiler. The experimental boiler is a small-scale direct-flow gas boiler equipped with a non-premixed burner, with specifications as detailed in Table 3.

Table 3. Boiler Specification Parameters

Model	LSS0.1-0.09-YQ
Evaporation Rate	0.1t/h
Outlet Steam Pressure	0.09MPa
Outlet Steam Temperature	112°C
Feedwater Temperature	25°C

(2) Boiler Performance Indicators

1. Heat Release Rate

The heat release rate is defined as the ratio of

the energy released by the fuel oxidation reaction in the furnace to the lower heating value of the fuel. The calculation formula is as follows:

$$\eta_c = \frac{Q_r}{Q_f} \# \quad (6)$$

$$Q_f = V_f \times LHV_f \# \quad (7)$$

In the formula:

Q_r : represents the heat released by the fuel per unit time, in kJ/h;

Q_f : represents the heat value of the fuel supplied to the boiler per unit time, in kJ/h.

2. Blending ratio

For the experimental boiler, the blending ratio is defined as the volumetric flow ratio of the auxiliary mixed gas (hydrogen or DMG) in the total mixed gas, with the following calculation formula:

$$X = \frac{V_a}{V_a + V_m} \# \quad (8)$$

In the formula:

V_a : represents the volumetric flow rate of hydrogen or DMG in the mixed gas, m³/h;

V_m : represents the volumetric flow rate of the main gas in the mixed gas, m³/h;

For clarity and ease of expression in the following sections, the blending ratio of hydrogen is denoted sending ratio of DMG is denoted as X_{DMG} .

(3) Experimental Test Bench

The gas routing system is essentially made up of the NG gas line, DMG gas line, hydrogen gas line, thermal gas flow meter, and gas mixing buffer tank. The fuel gas exits the gas cylinders via the ball valve, pressure regulator, flow meter, and check valve before entering the gas buffer tank and finally the burner. Gas pressure and flow are controlled by altering the pressure regulator's opening along the gas line. Figure 5 and Figure 6 demonstrate the gas routing system.

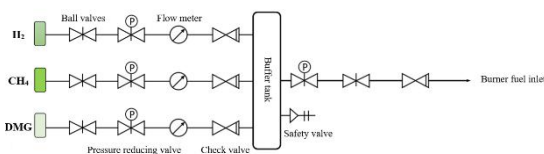


Figure 5. Schematic of the Gas Routing System

(4) Experimental Validation

The flow rate was set at 10 m³/h, with an excess air coefficient of 1.2. Experiments and simulations were carried out with natural gas as the fuel. Figure 7 shows the numerical

simulation results for the furnace temperature distribution. During the experiment, four thermocouples were placed into the furnace via the burner to detect temperature. Given that the furnace temperature exceeds the thermocouples' measuring range, the thermocouples were placed in cooler areas near the burner to ensure protection. Figure 8 shows the configuration of the thermocouples. Three thermocouples were installed beneath, to the left, and to the right of the burner, respectively. Each thermocouple was 0.3 m long, and their measurement spots were recorded on the temperature distribution cloud map derived from the numerical simulation results. Point A is beneath the burner, 0.27 m from the boiler casing; point B is to the left of the burner, 0.28 m from the boiler casing; and point C is to the right of the burner, also 0.28 m from the boiler casing.



Figure 6. Physical Image of the Gas Routing System

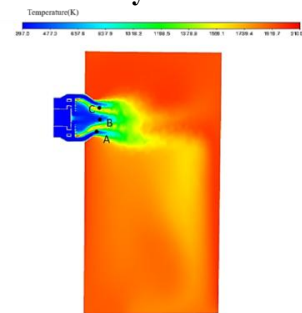


Figure 7. Furnace Temperature Contour Map

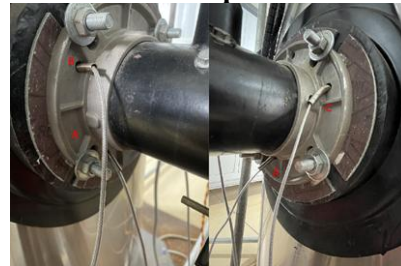


Figure 8. Thermocouple Temperature Measurement Points

Table 4 displays the experiment's measured and simulated temperature data. The findings show that the temperature values derived from

numerical calculations fluctuate close to the experimental values, with an error rate of less than 3%, which is within the permissible engineering range.

Table 4. Comparison of Experimental and Simulated Temperatures

	Location A (K)	Location B (K)	Location C (K)
Experiment	718	1170	1363
Numerical Calculation	734	1186	1378

3. The Impact of Hydrogen and Methanol Cracking Gas Blending Ratio on Natural Gas Combustion

The mixed fuel flow rate is set at 10m³/h, with an excess air ratio of 1.2 and a fuel inlet temperature of 340K. When configuring the fuel inlet boundary conditions, the volume fractions of hydrogen and DMG in the mixed gas are set to 5%, 10%, 15%, 20%, 25%, and 30%, respectively.

3.1 Heat Release Rate

Figure 9 depicts the variation in fuel heat release rate when natural gas is combined with hydrogen and DMG. The graph shows that when the hydrogen-to-DMG blending ratio increases, the heat release rate of the mixed fuel climbs and eventually falls. Specifically, when the hydrogen blending ratio is 5%, the heat release rate peaks at 94.87%, whereas when the DMG blending ratio is 10%, the heat release rate peaks at 94.76%. When the blending ratio is low, both hydrogen and DMG assist the full combustion of NG, resulting in a greater heat release. However, when the blending ratio is high, the combustion rate of hydrogen and DMG exceeds that of NG, causing stratification in the combustion process. Oxygen preferentially combines with hydrogen and DMG, reducing NG combustion, resulting in less heat emitted and a slower heat release rate.

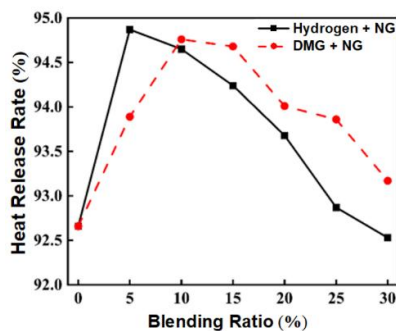


Figure 9. The Effect of Blending Ratio on Heat Release Rate

Overall, when the blending ratio is low, adding hydrogen has a bigger impact on increasing the heat release rate of the combined fuel. However, at greater blending ratios, the addition of DMG is more effective at increasing the heat release rate of the mixed fuel. This is because, during the combustion process, the hydrogen concentration of DMG has the greatest influence on the reaction.

3.2 Furnace Flue Gas Outlet Velocity

Figure 10 shows the variation in furnace exit velocity when NG is combined with hydrogen and DMG. The figure shows that as the mixing ratio of hydrogen and DMG increases, the furnace exit gas velocity drops. This is because, for the same volumetric flow rate, hydrogen and DMG require less air to complete combustion than NG, resulting in less heat. As a result, the flow rate of flue gas and pressure within the furnace are reduced after combustion.

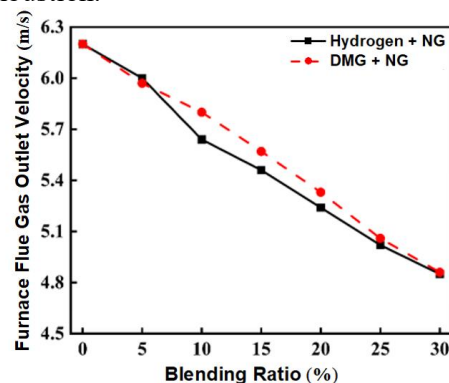


Figure 10. Effect of Blending Ratio on the Furnace Flue Gas Outlet Velocity

Hydrogen combustion produces simply water vapor, whereas complete combustion of DMG produces both water and carbon dioxide. Under identical temperature and pressure circumstances, carbon dioxide has a higher density than water vapor. Because the furnace exit is located below, the combustion products of DMG are more easily discharged. As a result, the flue gas exit velocity is slightly higher when NG is blended with DMG than when it is blended with hydrogen.

3.3 Distribution of Furnace Temperature.

3.3.1 The maximum temperature within the furnace

Figure 11 shows the variation in maximum furnace temperature when NG is mixed with hydrogen and DMG. The slope in the figure shows that mixing hydrogen and DMG

raises the maximum furnace temperature. As the blending ratio increases, the furnace temperature initially rises and then falls. The maximum temperatures, 2084 K and 2113 K are achieved with hydrogen and DMG mixing ratios of 20% and 15%, respectively. This is because the maximum furnace temperature is affected by both the heat emitted during combustion and the flame temperature. Although the combustion flame temperature of hydrogen and DMG is higher than that of NG, the amount of heat emitted per unit volume is less than half that of NG. Thus, when the mixing ratio is too low, the flame temperature does not reach its maximum, and when the mixing ratio is too high, the heat emitted during combustion is reduced. Overall, at low mixing ratios, DMG is more effective than hydrogen in increasing the maximum temperature. This is because the hydrogen in DMG increases the combustion rate; nevertheless, when compared to pure hydrogen, the combustion rate of DMG is more moderate, which aids in the regulation of flame length and temperature. Furthermore, DMG has a larger volumetric calorific value than hydrogen, allowing it to produce more heat when mixed in the same amount.

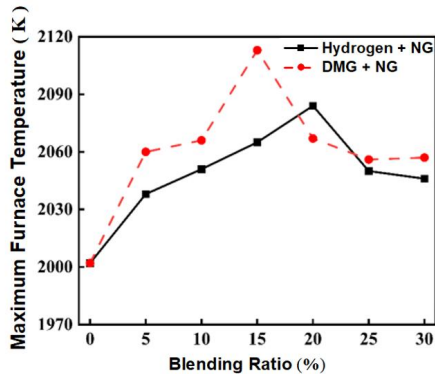


Figure 11. The Effect of Blending Ratio on the Maximum Furnace Temperature

3.3.2 The average furnace temperature.

Figure 12 shows the variation in average furnace temperature when NG is combined with hydrogen and DMG. The figure shows that combining hydrogen and DMG raises the average furnace temperature. As the mixing ratio increases, the furnace temperature rises dramatically, then falls slightly before stabilizing. The highest temperatures are attained when the hydrogen and DMG blend ratios reach 5%,

at 1886K and 1895K, respectively. This is because the average furnace temperature is determined by several factors, including the heat emitted during combustion, the reaction speed of the fuel, and the velocity of the exhaust gas exiting the furnace.

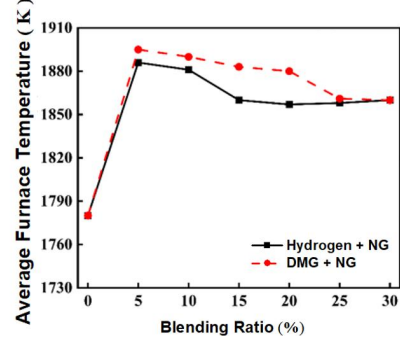


Figure 12. The Impact of Blending Ratio on the Average Furnace Temperature

At a lower mixing ratio, NG combustion is enhanced, resulting in more heat release. Meanwhile, the impact of hydrogen and DMG combustion speed on the overall combustion rate is negligible, resulting in relatively minor variations in the velocity of the flue gas at the furnace exit and an increase in average temperature. However, when the blending ratio increases, the heat generated by the combined fuel reduces, as does the velocity of flue gas at the furnace outlet. As a result, the average furnace temperature lowers, albeit little.

Overall, the average temperature rises when NG is blended with DMG rather than hydrogen. This is because of DMG's larger volumetric calorific value than hydrogen and the lesser amount of water vapor produced in the combustion products. Water vapor has a substantially higher specific heat capacity than carbon dioxide at the same condition, therefore the products absorb less heat from the fuel, resulting in a higher average furnace temperature.

3.3.3 Furnace flue gas outlet temperature.

Figure 13 depicts fluctuations in furnace outlet temperature when NG is mixed with hydrogen and DMG. As shown in the graph, the combination of hydrogen and DMG raises the furnace's average temperature. As the mixing ratio increases, the furnace temperature rises dramatically before marginally decreasing. When the hydrogen mixing ratio is 5%, the furnace outlet temperature peaks at 1988 K, but when the DMG mixing ratio is 15%, the highest

outlet temperature is 2011 K. This is because the furnace output temperature is controlled by the heat released by the fuel as well as the length of time the flue gas remains in the furnace. At a low mixture ratio, NG combustion is improved, resulting in an increase in heat output and a higher furnace outlet temperature. However, when the mixing ratio increases, the amount of heat emitted by the mixed fuel decreases. Furthermore, the quick burning of hydrogen and DMG produces fewer product components, shortening the residence time of the flue gas in the furnace, and resulting in insufficient heat exchange at various points inside the furnace and a lower output temperature.

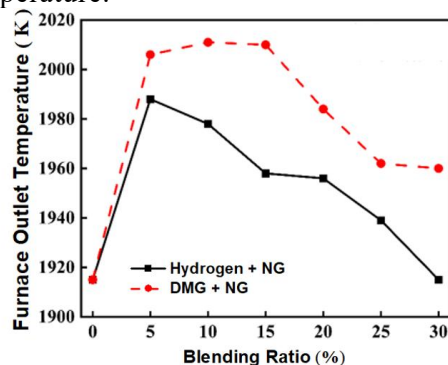


Figure 13. The Impact of Blending Ratio on Furnace Outlet Temperature

Overall, when NG is combined with DMG, the furnace outlet temperature rises above that of hydrogen. In addition to hydrogen, DMG largely comprises carbon monoxide, which leads to more complex combustion products. This intricacy improves fluid flow and turbulence, which increases convective heat transfer. Furthermore, DMG has a larger volumetric heat value than hydrogen, which contributes to the higher output temperature observed when DMG is blended.

4. Conclusion

This study developed a three-dimensional model of a small-scale direct-current boiler, calibrated through experimental validation, to investigate variations in key parameters such as heat release rate, flue gas outlet velocity, and furnace temperature distribution after blending NG with hydrogen and DMG. The detailed results are as follows:

(1) The modeling, mesh production, and

calculation of beginning and boundary conditions for the experimental boiler have been accomplished. The numerical model was calibrated with NG combustion experimental data, and mesh independence was confirmed. The optimum mesh count model was finalized for future research.

(2) Blending hydrogen and DMG increased the heat release rate, maximum furnace temperature, average furnace temperature, and furnace outlet temperature of NG while decreasing the flue gas outlet velocity. At a hydrogen blending ratio of 5%, the heat release rate increased by a maximum of 2.2%, while the average furnace temperature peaked at 1886 K. At a 10% methanol cracking gas blending ratio, the heat release rate rose by up to 2.1%, while at a 5% blending ratio, the average furnace temperature reached its maximum of 1895 K. Hydrogen showed a greater improvement in the heat release rate of NG combustion, although DMG was more successful in increasing furnace temperature.

References

- [1] Liu J, Zhuang Y, Wang C, et al. Life cycle carbon footprint assessment of coal-to-SNG/methanol polygeneration process. *Science of The Total Environment*, 2024, 908: 168409.
- [2] Wang X, Demirel Y a. Feasibility of power and methanol production by an entrained-flow coal gasification system. *Energy & Fuels*, 2018, 32(7): 7595-7610.
- [3] Tian Z, Wang Y, Zhen X, et al. The effect of methanol production and application in internal combustion engines on emissions in the context of carbon neutrality: A review. *Fuel*, 2022, 320: 123902.
- [4] Impacts of methanol fuel on vehicular emissions: A review. *Frontiers of Environmental Science & Engineering*, 2022, 16(9).
- [5] Gu Y, Wang D, Chen Q, et al. Techno-economic analysis of green methanol plant with optimal design of renewable hydrogen production: A case study in China. *International Journal of Hydrogen Energy*, 2022, 47(8): 5085-5100.
- [6] Crivellari A, Cozzani V, Dincer I. Exergetic and exergoeconomic analyses of novel methanol synthesis processes driven by offshore renewable energies. *Energy*,

- 2019, 187.
- [7] X. Z. Liu, G. Y. Zhu, T. Asim, R. Mishra. Combustion characterization of hybrid methane-hydrogen gas in domestic swirl stoves. *Fuel*, 2023, 333: 126413
- [8] D. T. Balanescu, V. M. Homutescu. Effects of hydrogen-enriched methane combustion on latent heat recovery potential and environmental impact of condensing boilers. *Applied Thermal Engineering*, 2021, 197: 117411
- [9] M. X. Sun, X. M. Huang, Y. L. Hu, S. Lyu. Effects on the performance of domestic gas appliances operated on natural gas mixed with hydrogen. *Energy*, 2022, 244: 122557
- [10] Ali A, Shaikh M N. Recent developments in catalyst design for liquid organic hydrogen carriers: Bridging the gap to affordable hydrogen storage. *International Journal of Hydrogen Energy*, 2024, 78: 1-21.
- [11] Jiang Yankun. Alcohol-Hydrogen Automotive Technology and Its Power System. *Proceedings of the 2017 International Clean Energy Forum*. Macau, 2017: 257-275.
- [12] Jiang Y, Chen Y, Xie M. Effects of blending dissociated methanol gas with the fuel in gasoline engine. *Energy*, 2022, 247.
- [13] Guban D, Muritala I K, Roeb M, et al. Assessment of sustainable high temperature hydrogen production technologies. *International Journal of Hydrogen Energy*, 2020, 45(49): 26156-26165.
- [14] Chen Y, Jiang Y, Zhang B, et al. Impact of preparation methods on the performance of Cu/Ni/Zr catalysts for methanol decomposition. *Materials Research Express*, 2024, 11(2).
- [15] Liu Bin. *Fluent 19.0 Fluid Simulation: From Beginner to Master*. Beijing: Tsinghua University Press, 2019.